JOURNAL OF PROPULSION AND POWER
Vol. 24, No. 5, September–October 2008

Technical Notes

TECHNICAL NOTES are short manuscripts describing new developments or important results of a preliminary nature. These Notes should not exceed 2500 words (where a figure or table counts as 200 words). Following informal review by the Editors, they may be published within a few months of the date of receipt. Style requirements are the same as for regular contributions (see inside back cover).

Electromagnetic Flow Sensor for Liquid-Metal-Fed Electric Propulsion

Kurt A. Polzin,* Thomas E. Markusic,† Boris J. Stanojev,‡
Chris Dodson,§ and Amado DeHoyos¶
NASA Marshall Space Flight Center,
Huntsville, Alabama 35812

DOI: 10.2514/1.35329

Nomenclature

B	=	magnetic induction, T
E	=	electric field, V/m
l, s, w	=	lengths, m
$\dot{m}$	=	mass flow rate, kg/s
t	=	time, s
u	=	flow velocity, m/s
V	=	voltage, V
$\dot{\mathcal{V}}$	=	volumetric flow rate, m^3/s

I. Introduction

LIQUID metals have been used as propellants in almost all major categories of electric propulsion (EP) devices. These have included lithium-fed arcjets [1], lithium- [2] and gallium-fed [3] magnetoplasmadynamic (MPD) thrusters, bismuth-fed Hall thrusters [4,5], and mercury- [6,7], cesium- [8,9], and indium-fed [10] electrostatic thrusters [both ion engines and field emission electric propulsion (FEEP)]. The use of liquid-metal propellants in high-power Hall and MPD thrusters has recently been investigated as a potentially promising path toward the development of high-performance, long-lifetime electric thrusters [4,11]. The ability to accurately control and measure small liquid-metal propellant flow rates [$\mathcal{O}$(10–100) mg/s] is necessary to assess the performance of thrusters in a laboratory environment; flight-rated flow systems will have the added demands of high-reliability and low system mass. Typical flow rates obtained various liquid-metal-fed EP thrusters are presented in Table 1. We observe from the table that the target mass flow rate of 10–100 mg/s represents flows found only in higher power EP systems.

Since the 1960s, there have been a number of different techniques developed to measure the mass flow rates in these liquid-metal thruster systems. Mass flow rates in mercury ion thrusters have been measured using 1) a calorimetric technique, where the difference between two temperature measurements was correlated through calibration to the mass flow rate [15], 2) a capillary flow impedance technique, where a differential pressure measurement was performed between the ends of a long (~10 m) capillary tube and correlated to the rate of displacement of a piston in a reservoir [7], and 3) a pressure-head technique, where the height of a column of propellant was optically recorded and compared with the theoretical height for a given mass flow rate [16]. In addition, the flow rate in a lithium-fed Lorentz force accelerator has been measured by monitoring the displacement of the piston used to force propellant into the thruster [2].

In this Note, we address the problem of attaining high measurement accuracy at low mass flow rates, deferring the material compatibility issues associated with high-temperature reactive propellants to later studies. Tests were performed using gallium, which possesses a low melting temperature, is nonreactive with many materials, including plastics and polymers, and is nontoxic. We demonstrate an electromagnetic flow sensor that can accurately measure the propellant mass flow rate at levels commensurate with operation of an electric thruster.

II. Sensor Theory

The principle of operation of an electromagnetic (EM) flow sensor (see Fig. 1) derives from Faraday's law: when an electrically conductive medium (a conductive liquid in the present case) moves transverse to an applied magnetic field, a "back-emf" is induced according to

$$\mathbf{E} = -\mathbf{u} \times \mathbf{B}$$

Assuming that the magnetic field and velocity are homogeneous throughout the cavity, integration over the channel width w yields an induced voltage equal to

$$V = uBw$$

which is independent of the properties of the conducting fluid. In Fig. 1, $u = \dot{m}/(\rho s w)$, where $\dot{m}$ is the mass flow rate, ρ is the fluid density, and s is the channel height. The net induced voltage expressed as a function of mass flow rate is

$$V = \frac{B}{s}\frac{\dot{m}}{\rho} \tag{1}$$

Replacing the mass flow rate with the volumetric flow rate $\dot{\mathcal{V}}$ allows us to write the induced voltage as

$$V = \frac{B}{s}\dot{\mathcal{V}} \tag{2}$$

The parameter B/s is important in determining the performance of an EM flow sensor. The output voltage, and hence the ultimate resolution, of the flow sensor increases linearly with B/s for a given mass flow rate and fluid density (or a given volumetric flow rate).

Received 26 October 2007; revision received 14 April 2008; accepted for publication 18 June 2008.

*Propulsion Research Engineer, Propulsion Research and Technology Applications Branch, Propulsion Systems Department. Senior Member AIAA.

†Research Scientist; currently Director, Texas Test Site, Space Exploration Technologies, Inc., El Segundo, CA 90245.

‡Senior Research Engineer, Madison Research Corporation, Huntsville, AL 35805; currently Propulsion Manager, Swedish Space Corporation, Stockholm, Sweden. Member AIAA.

§Undergraduate Student Research Program; currently Propulsion Test Engineer, Space Exploration Technologies, Inc., El Segundo, CA 90245.

¶Summer Research Assistant; currently Propulsion Test Engineer, Space Exploration Technologies, Inc., El Segundo, CA 90245.

Table 1 Order of magnitude mass flow rate ranges for various liquid-metal-fed electric propulsion systems

System	$\dot{m}$ range	Power level
Indium FEEP [10]	<1–10 μg/s	~0.1–10 W
Cesium FEEP [9]	<1–10 μg/s	~0.1–10 W
Mercury ion [12]	0.1–10 mg/s	~4 kW
Cesium ion [13]	1–10 mg/s	~0.5–3 kW
Bismuth Hall [14]	0.1–10 mg/s	25–36 kW
Lithium MPD [2]	10–100 mg/s	30–200 kW

Calibration of the flow sensor provides a measure of the time-independent term B/s, simplifying the use of the sensor because the output voltage then scales linearly with the volumetric flow rate. Using permanent magnets, the values of B/s cannot exceed the range of 10–100 T/cm. For these values of B/s and gallium mass flow rates from 10–100 mg/s, the theoretical output of an EM flow sensor is on the order of 1–100 μV.

III. Proof-of-Concept Experiment

An exploded view and a photograph of a prototype liquid-metal (gallium) EM flow sensor are shown in Figs. 2a and 2b, respectively. The magnetic circuit consists of a pair of samarium cobalt magnets and an iron yoke that contains the flux. The liquid gallium flows within a polycarbonate insulating body, which has a channel height s of 0.025 cm (0.010 in.). The magnets are insulated from the gallium by a polycarbonate layer measuring 0.025 cm (0.010 in.), resulting in a total separation between the faces of the magnet of 0.076 cm (0.030 in.). This configuration produced a calculated on-axis field strength of 0.9 T, resulting in a B/s ratio of ~35 T/cm. Stainless steel feed lines deliver gallium to the sensor, and gold-plated tungsten electrodes are used to measure the induced back-emf across the channel.

The EM flow sensor was tested in a flow loop capable of providing continuous, steady flow measurements in a closed-loop configuration, or flow rate calibration measurements performed in an open-loop configuration. For both closed- and open-loop operation, the liquid gallium was electromagnetically pumped [17] through the loop. In addition, in the open-loop configuration, there was a time-changing gravitational pressure head that helped force liquid gallium through the loop. During calibration, gallium was discharged from the flow loop into a catch basin, where its accumulation was measured as a function of time using a precision Sartorius GC2502 scale (0.001 g resolution). In both the closed-loop and open-loop configurations, the flow sensor output voltage was measured using a Keithly 2701 multimeter (0.1 μV resolution).

IV. Results

EM flow sensor calibration data obtained while operating in the open-loop configuration are presented in Fig. 3. The top graph shows the induced voltage measured across the flow sensor, whereas the bottom graph shows the total mass accumulated in the catch basin as a function of time. The total hydrostatic pressure head due to gravity decreases over time as the gallium liquid level in the reservoir drops, leading to a reduction over time in the flow rate through the sensor. The mass flow rate was obtained by numerically differentiating the accumulated mass with respect to time, taking into account the changing hydrostatic pressure. These data are plotted as a function of flow sensor voltage in Fig. 4. A linear curve fit provides a measure of the constant relating mass flow rate to the induced voltage across the flow sensor. A quick calculation of the theoretical sensor output as given by Eq. (1) shows that $\rho(B/s)^{-1}$ is ~1690 g/(sV), which is the

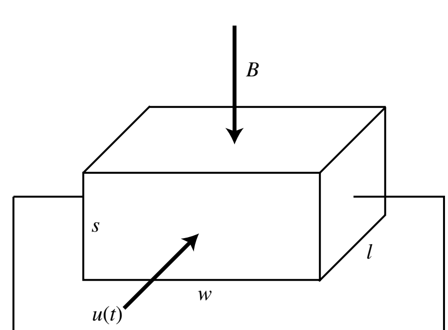

Fig. 1 Idealized schematic of an electromagnetic flow sensor.

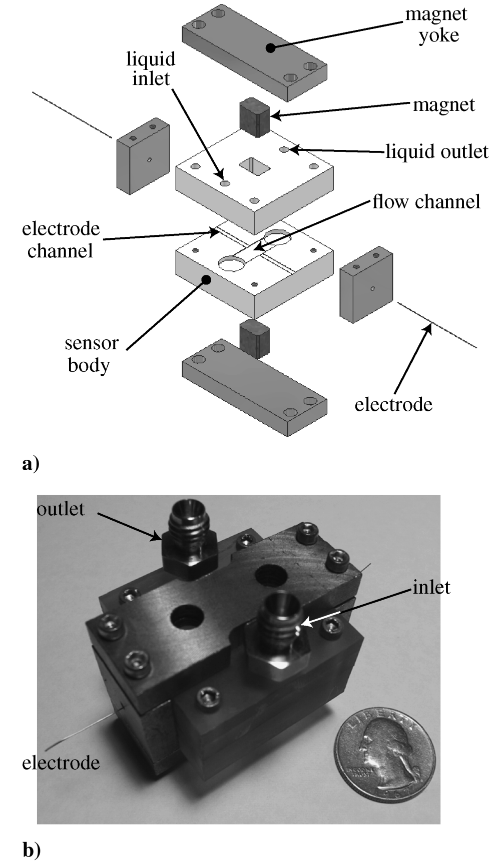

Fig. 2 EM flow sensor: a) exploded CAD solid model and b) photograph of assembled device.

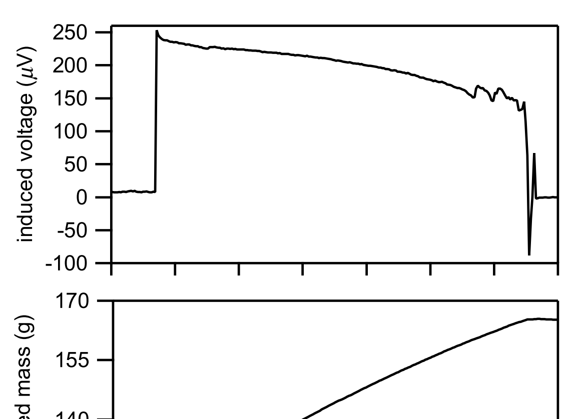

Fig. 3 Open-loop calibration data for the EM flow sensor: a) voltage (back-emf) induced in the EM flow sensor by the flowing gallium, and b) mass of gallium pumped through the system and accumulated on a scale.

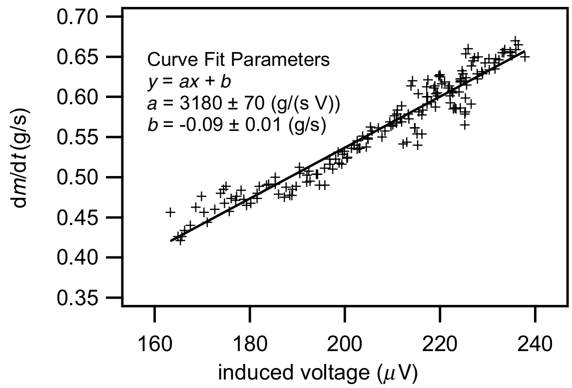

Fig. 4 Open-loop calibration data for the EM flow sensor. Data points indicate mass flow rate (time derivative of Fig. 3b plotted against the measured back-emf from Fig. 3a). Line indicates linear curve fit of the data set giving the mass flow rate dm/dt as a function of back-emf.

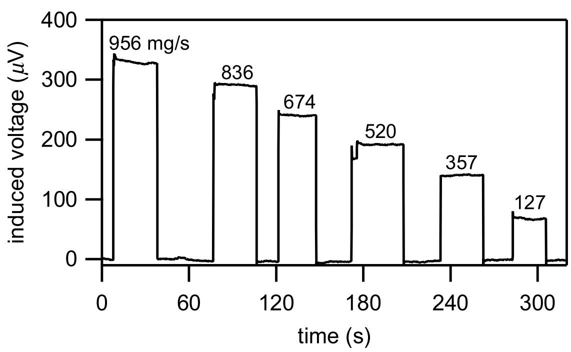

Fig. 5 Measured back-emf produced by closed-loop flow of gallium through the EM flow sensor. The gallium mass flow rate is calculated using the calibration curve given in Fig. 4.

same order of magnitude as the curve-fit slope a. The discrepancy in values is most likely due to the assumptions in the theoretical treatment that the magnetic field and velocity profiles are homogeneous throughout the cavity.

In closed-loop operation, various flow rates were produced by operating the EM pump at different current levels. The current through the pump was held constant until the flow rate measurement indicated that the flow had reached an approximate steady-state level. The current through the pump was then returned to zero before initiating a subsequent trial. The induced voltages measured by the flow sensor as a function of time are presented in Fig. 5. The mass flow rates displayed above each voltage plateau were computed using the calibration coefficients found from the curve fit in Fig. 4. The measured voltage at the highest flow rate was approximately 330 μV. The estimated error on the flow rate measurement is $\sim$5.4%, which represents a combination of both the random uncertainty in the measurement and the uncertainty in the calibration coefficients.

V. Conclusions

We have demonstrated that an EM flow sensor is capable of performing high-accuracy measurements on liquid metals at typical flow rates found in electric thrusters. Theoretical analysis shows that the induced voltage, and consequently the sensor resolution, can be increased by increasing the ratio of B/s. However, the practical limits on the size of this ratio limit the voltage output of the flow sensor to the order of 10–100 μV for flow rates of interest in electric propulsion applications. Induced voltages obtained during flow sensor calibration with liquid gallium agree in order of magnitude with these predictions and demonstrate the linear dependence between the back-emf and the mass flow rate. In proof-of-concept experiments, gallium mass flow rates ranging from 125 to 950 mg/s were successfully measured using a prototype EM flow sensor. The estimated error on these measurements was roughly 5%. Although the sensor was tested using gallium, for an application like a lithium-fed MPD, this sensor would actually have a sensitivity approximately an order of magnitude better than the results presented in this note because the density of gallium is slightly more than an order of magnitude greater than that of lithium.

Acknowledgments

The authors appreciate the continued support of Jim Martin and Michael LaPointe. This work was supported by NASA's Exploration Systems Mission Directorate and performed under contract NNM05AA25C, managed by Randy Baggett.

References

[1] Connolly, D. J., Sovie, R. J., Michels, C. J., and Burkhart, J. A., "Low Environmental Pressure MPD Arc Tests," *AIAA Journal*, Vol. 6, No. 7, 1968, pp. 1271–1276.
doi:10.2514/3.4733

[2] Kodys, A. D., Emsellem, G., Cassady, L. D., Polk, J. E., and Choueiri, E. Y., "Lithium Mass Flow Control for High Power Lorentz Force Accelerators," *AIP Conference Proceedings*, Vol. 552, No. 1, 2001, pp. 908–915.
doi:10.1063/1.1358027

[3] Thomas, R. E., Burton, R. L., Glumac, N. G., and Polzin, K. A., "Preliminary Spectroscopic Measurements for a Gallium Electromagnetic (GEM) Thruster," AIAA Paper 2007-5855, July 2007.

[4] Tverdokhlebov, S. O., Semenkin, A. V., and Polk, J. E., "Bismuth Propellant Option for Very High Power TAL Thruster," AIAA Paper 2002-348, Jan. 2002.

[5] Sengupta, A., Marrese-Reading, C., Cappelli, M., Scharfe, D., Tverdokhlebov, S., Semenkin, S., Tverdokhlebov, O., Boyd, I., Keidar, M., Yalin, A., Surla, V., Markusic, T., and Polzin, K., "Overview of the VHITAL Program: A Two-Stage Bismuth Fed Very High Specific Impulse Thruster with Anode Layer," *International Electric Propulsion Conference*, Electric Rocket Propulsion Society Paper 2005-238, Oct. 2005.

[6] King, H. J., Molitor, J. H., and Kami, S., "System Concepts for a Liquid Mercury Cathode Thruster," AIAA Paper 1967-699, Sept. 1967.

[7] Hyman, J., Jr., Bayless, J. R., Schnelker, D. E., Ward, J. W., and Simpkins, J., "Development of a Liquid-Mercury Cathode Thruster System," *Journal of Spacecraft and Rockets*, Vol. 8, No. 7, 1971, pp. 717–721.
doi:10.2514/3.59717

[8] Collett, C. R., Dulgeroff, C. R., and Simpkins, J. M., "Cesium Microthruster System," AIAA Paper 1969-292, March 1969.

[9] Marcuccio, S., Genovese, A., and Andrenucci, M., "Experimental Performance of Field Emission Microthrusters," *Journal of Propulsion and Power*, Vol. 14, No. 5, 1998, pp. 774–781.

[10] Tajmar, M., Genovese, A., and Steiger, W., "Indium Field Emission Electric Propulsion Microthruster Experimental Characterization," *Journal of Propulsion and Power*, Vol. 20, No. 2, 2004, pp. 211–218.
doi:10.2514/1.9247

[11] Gorshokov, O. A., Shutov, V. N., Kozubsky, K. N., Ostrovsky, V. G., and Obukhov, V. A., "Development of High Power Magnetoplasmadynamic Thrusters in the USSR," *International Electric Propulsion Conference*, Electric Rocket Propulsion Society Paper 2007-136, Sept. 2007.

[12] King, H. J., Eckhardt, W. O., Ward, W., and Knechtli, R. C., "Electron-Bombardment Thrusters Using Liquid-Mercury Cathodes," AIAA Paper 1966-232, March 1966.

[13] Speiser, R. C., Reid, G., and Sohl, G., "Cesium Electron Bombardment Ion Engines," AIAA Paper 1965-373, July 1965.

[14] Marrese-Reading, C., Swindlehurst, R., Owens, A., Markusic, T., Polzin, K., Knowles, T., and Mueller, J., "Development of a Bismuth Feed System for the Very High Isp Thruster with Anode Layer (VHITAL) Program," AIAA Paper 2006-4635, July 2006.

[15] Pye, J. W., "Component Development for a 10 cm Mercury Ion Thruster," AIAA Paper 1972-487, April 1972.

[16] Kerslake, W. R., "Design and Test of Porous-Tungsten Mercury Vaporizers," AIAA Paper 1972-484, April 1972.

[17] Polzin, K. A., and Markusic, T. E., "Electromagnetic Pumps for Liquid Metal-Fed Electric Thrusters," *Journal of Propulsion and Power*, Vol. 23, No. 6, 2007, pp. 1285–1290.
doi:10.2514/1.30819

E. Choueiri
Associate Editor